

Effect of Spin Fluctuations on Phonon-Mediated Superconductivity in the Vicinity of a Quantum Critical Point

Y. L. Loh

Department of Physics, Purdue University, West Lafayette, IN 47907

P. B. Littlewood

Theory of Condensed Matter Group, Cavendish Laboratory,
University of Cambridge, Madingley Road, Cambridge CB3 0HE, United Kingdom
(Dated: April 15, 2024)

We consider an s-wave superconductor in the vicinity of a second-order ferromagnetic (FM) or spin-density-wave (SDW) quantum critical point (QCP), where the superconductivity and magnetism arise from separate mechanisms. The quantum critical spin fluctuations reduce the superconducting T_c . Near a FM QCP, we find that T_c falls to zero as $1/\ln(1/\xi)$ in 3D and as $1/\xi$ in 2D, where $1/\xi = J/J_c$ is the inverse correlation length of the spin fluctuations, and ξ measures the distance $1/\xi = J/J_c$ from the quantum critical point. SDW quantum critical fluctuations, on the other hand, suppress T_c to zero as $1/\xi$ in 2D, and suppress T_c only to a finite value in 3D, producing a cusp of the form $\text{const} + 1/\xi$.

PACS numbers:

I. INTRODUCTION

There has been much interest recently in the interplay of superconductivity and magnetic phenomena. Many different scenarios arise depending on the superconducting pairing symmetry (singlet/triplet, s/p/d-wave)³⁹ and the type of magnetism (static/fluctuating ferromagnetism/antiferromagnetism/spin density waves). Much attention has been given to magnetically-mediated unconventional superconductivity, such as models of d-wave singlet superconductivity driven by antiferromagnetic spin fluctuations (possibly applicable to the cuprates and heavy-fermion superconductors¹), and p-wave-like triplet pairing in $\text{He}^{32,3}$, Sr_2RuO_4 ⁴ and UGe_2 ^{5,6} driven by ferromagnetic spin fluctuations.

However, there are of course systems where conventional s-wave pairing coexists with magnetism. While the coexistence of antiferromagnetic or SDW order with superconductivity is not uncommon, the coexistence of FM with s-wave superconductivity is rare. In ErRh_4B_4 ⁷ and HoMgO_6S_8 ^{8,9}, magnetism and superconductivity arise from independent mechanisms (RKKY coupling between f-electrons and phonon exchange respectively). It is now well accepted that static magnetic order has a pair-breaking effect on BCS singlet s-wave superconductivity (as does any perturbation which breaks time-reversal symmetry), often resulting in the complete destruction of superconductivity. The mean-field theory of ferromagnetic superconductors was studied by Gor'kov and Rusinov¹⁰, although a more general analysis suggests a Larkin-Ovchinnikov-Fulde-Ferrell state with a non-uniform order parameter^{11,12}. A mean-field theory based on a simple 'Hestings-fraction' model (similar to that of Bilbro and Millan¹³ for the coexistence of charge-density-wave order and superconductivity) shows that coexistence of spin-density-wave (SDW) order and superconducting order may also be possible in a limited range

of parameters¹⁴.

One expects that magnetic fluctuations should also have a pair-breaking effect on s-wave superconductivity, especially for a system close to a second-order magnetic QCP, where the amplitude of the fluctuations becomes very large. Berk and Schrieffer¹⁵ showed numerically that in the presence of ferromagnetic fluctuations a finite electron-phonon coupling V_{ph} is required to produce superconductivity, and in Pd, for example, this critical coupling is so large that superconductivity does not occur at all. We study this problem in more detail, obtaining analytic results for the dependence of T_c as the QCP is approached.

We assume that the pairing interaction is due to phonon exchange, and can be represented by a BCS interaction, whereas the magnetism is driven by a coupling J between itinerant electrons or localized spins such that when J exceeds a critical coupling J_c at $T = 0$ the system undergoes a second-order phase transition from a disordered state to a magnetically ordered state. The resulting interaction between electron spins (as a function of Matsubara frequency $i\omega_n$) is assumed to be of the Hertzian form

$$V_{nq}^s = \frac{J_0^2}{2 + q^2 + \frac{j_{\parallel n}^2}{q}} \quad \text{or} \quad \frac{J_0^2}{2 + \frac{j_{\parallel n}^2}{Q^2} + \frac{j_{\perp n}^2}{q}} \quad (1)$$

near a FM (SDW) QCP. Here $1/\xi$ is the diverging correlation length. This approach is similar to the fluctuation-exchange (FLEX) approach used by Monthoux¹⁶ to study spin-fluctuation-mediated d-wave-like superconductivity, and to that of Wang et al.¹⁷ and Roussev and Millis¹⁸, who studied a model of p-wave pairing where the ferromagnetic fluctuations suppressed T_c to a finite value at the QCP. Also, Li et al.¹⁹ have performed related studies of the electromagnetic properties of superconductors near ferromagnetic instabilities.

As the QCP is approached, the energy scale of the spin fluctuations goes to zero ('critical slowing down') and their amplitude goes up. We show that in the vicinity of the quantum critical point, pair-breaking by slow spin fluctuations can be mapped onto the Abrikosov-Gorkov problem of pair-breaking by static magnetic impurities. We thus predict that T_c may or may not be suppressed all the way to zero at the QCP, depending upon the dimensionality and the type of magnetism:

2D FM	T_c	$p - \frac{J}{J_c}$	$\propto J$
2D SDW	T_c	$\frac{J}{J_c}$	$\propto J^2$
3D FM	T_c	$1 - \ln(1 - \frac{J}{J_c})$	$1 - \ln(1 - \frac{J}{J_c})$
3D SDW	T_c	$\text{const} + \frac{J}{J_c}$	$\propto J$

where ν is the correlation length exponent. We expect these forms to apply on both sides of the transition.

II. CHARGE-CHARGE INTERACTION

Starting with an electron-phonon Hamiltonian, integrating out the phonons in the harmonic approximation, and making certain approximations for the structure of the electron-phonon coupling in momentum space leads to the following action for phonon-mediated superconductivity:

$$S[\psi; \psi^\dagger] = T \sum_n \sum_k (i\epsilon_n - \epsilon_k) \psi_{nk}^\dagger \psi_{nk} + \frac{1}{2} V^c \sum_{\mathbf{x}, \mathbf{x}'} \psi_{\mathbf{x}}^\dagger \psi_{\mathbf{x}'} \psi_{\mathbf{x}} \psi_{\mathbf{x}'} \quad (2)$$

where $\epsilon_n = 2\pi(n + \frac{1}{2})T$ are fermionic Matsubara frequencies, $\epsilon_k = \frac{1}{2}$ is a spin index, ϵ_k is the electron dispersion relation, \mathbf{x} runs from 0 to $\mathbf{x} = 1/T$, $\psi_{\mathbf{x}} = \frac{1}{2} \sum_{\mathbf{k}} \psi_{\mathbf{k}} \psi_{-\mathbf{k}}$ is the electron density operator, and V^c is an effective interaction in the 'charge' channel that is second order in the electron-phonon coupling g and first order in the phonon propagator D . If the superconductivity is isotropic and the Fermi surface is spherical, or if the system is dirty enough that the order parameter is effectively averaged over the Fermi surface, then for the purpose of calculating superconducting properties V_{nq}^c (the Fourier transform of $V_{\mathbf{x}}^c$) can be replaced by an effective interaction V_n^c in the Eliashberg equations. V_n^c is usually referred to in the literature as $\lambda^2 F^n$, and is obtained by averaging the interaction V_{nq}^c over pairs of momenta on the Fermi surface²⁰:

$$V_n^c = \frac{1}{\Omega_F} \int_{\mathbf{k}, \mathbf{p}} (k) (p) V_{nkp}^c = \frac{1}{\Omega_F} \int_{\mathbf{k}} (k) V_{nk}^c \quad (3)$$

where $\int_{\mathbf{k}} = \int \frac{d^d k}{(2\pi)^d}$ is an integral over the Brillouin zone. Note that $\int_{\mathbf{k}} (k) = \int_S \frac{d^d k}{(2\pi)^d v_F}$, where the integral is performed over the Fermi surface, weighted by the inverse Fermi velocity $1/v_F(k)$, where $v_F(k) = \frac{\partial \epsilon(k)}{\partial k}$.

III. EFFECT OF FM FLUCTUATIONS ON T_c

A. Spin-spin interaction V_{nq}^s near a FM-QCP

In the random phase approximation (RPA), the spin correlation function in an itinerant ferromagnet has the following form at small n and q :

$$\chi_{nq} = \frac{\chi_0^2}{2 + q^2 + \frac{J_n^2}{q}} \quad (4)$$

where χ_0 , the inverse spin-fluctuation correlation length in the interacting system, is reduced from its bare value χ_0^0 as $\chi_0 = \chi_0^0 (1 - J/J_c) = 1/\nu$ with $\nu = 1/2$, so that undergoes Stoner enhancement. J indicates the 'distance' from the ferromagnetic quantum critical point (QCP); a second-order quantum phase transition occurs at $J = J_c$, when $\nu = 0$. Eq. (4) can also be obtained by integrating out the electrons to obtain a Landau-Ginzburg-Wilson effective action for a spin field.

For a long time it was thought that low-energy long-wavelength quantum fluctuations are irrelevant ($\nu > 1$) so that Eq. (4) is universally true²¹. However, there is growing evidence that these 'soft modes' are actually relevant, changing the form of χ or even causing the second-order QCP to become weakly first order^{22,23,24}. In this paper we restrict ourselves to regimes in which such effects are negligible, so that Eq. (4) holds, albeit for some ν not necessarily equal to $1/2$.

This form for χ leads to an effective spin-spin interaction

$$V_{nq}^s = \frac{J_0^2}{2 + q^2 + \frac{J_n^2}{q}} \quad (5)$$

which diverges at small J_n and q as $J \rightarrow J_c$; these large spin fluctuations are likely to have an important effect on superconductivity.

Eq. (5) is a generic expression for the spin-spin interaction near any kind of ferromagnetic QCP, and should be applicable regardless of whether the ferromagnetism and superconductivity arise from a single band of itinerant electrons or from different bands (or even if the magnetism is due to localized spins, provided that one can find a model of localized spins that exhibits a second-order quantum phase transition).⁴⁰ Ultimately, the spin-fluctuation-mediated interaction can be represented by a low-energy effective action of a form analogous to Eq. (2):

$$S_e^{\text{spin}}[\psi; \psi^\dagger] = \frac{1}{2} V^s \sum_{\mathbf{x}, \mathbf{x}'} \psi_{\mathbf{x}}^\dagger \psi_{\mathbf{x}'} S_{\mathbf{x}} S_{\mathbf{x}'} \quad (6)$$

B. Jacobian J_q for spherical Fermi surface

The dimensionless effective spin-spin interaction, V_n^s , may be calculated in the same way as the effective

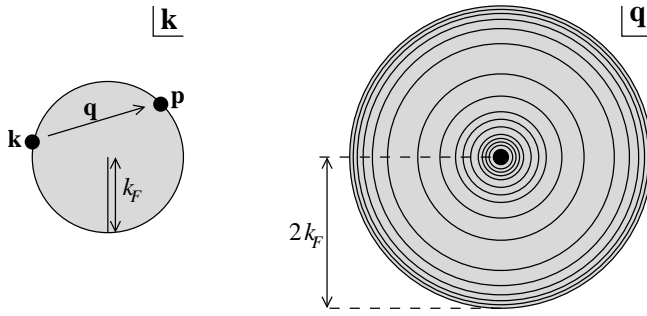


FIG. 1: (Left) 2D circular Fermi surface in k -space. (Right) contours of q (schematic).

phonon-mediated attraction in Eq. (3):

$$V_n^s = \int_{k,p} \int_k \int_q \frac{V_{n,k,p}}{q} V_{n,q}^s \quad (7)$$

where q is a Jacobian corresponding to the change of variables, which is the autocorrelation of the Fermi surface:

$$q = \int_k \int_{k+q} \int_k \int_k : \quad (8)$$

can be calculated geometrically in 2D (3D) by considering the areas (volumes) of intersection of circular annuli (spherical shells). The results are

$$q = \frac{m}{q k_F} \left(1 - \frac{q}{2k_F} \right)^2 \quad (2D); \quad (9)$$

$$q = \frac{m}{2q k_F} \left(1 - \frac{q}{2k_F} \right) \quad (3D); \quad (10)$$

Both these expressions are normalized such that $\int_q q = R$. In both 2D and 3D, it can be shown that q goes as $1=q$ near $q = 0$. In both 2D and 3D this, by itself, is an integrable singularity. However, when $\omega = 0$ and $\epsilon_n = 0$, $V_{n,q}^s$ goes as $1=q^2$ near $q = 0$. The entire integrand of Eq. (7) thus goes as $1=q^3$. We shall show that this makes the integral divergent.

C. Effective interaction V_n^s near FM-QCP

For the case of a 2D circular Fermi surface, substituting Eq. (9) into (7) gives

$$V_n^s = \frac{m J_0^2}{2^2 k_F^2} \int_0^{2k_F} dq \frac{1}{q^2 + \omega^2 + \frac{j_n j}{q}} \quad (11)$$

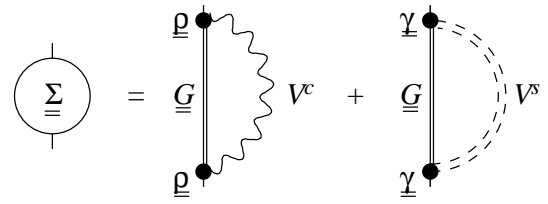


FIG. 2: Diagrams for the matrix self-energy.

where \int_n is the 2D density of states.⁴¹ V_n^s diverges as $1=n^3$, and is cut off for $1_n < n^3$, at a value of the order of $1=n$. For a 3D spherical Fermi surface, substituting Eq. (10) into (7) gives

$$V_n^s = \frac{m J_0^2}{4^2 k_F^2} \int_0^{2k_F} dq \frac{q}{q^2 + \omega^2 + \frac{j_n j}{q}} \quad (12)$$

with logarithmic accuracy for small, positive 1_n . Here \int_n is the 3D density of states. The integrand has a divergence cut off by 1_n and 1_n^2 . V_n^s diverges as $\ln 1=n$, and is cut off for $1_n < n^3$, at a value of the order of $\ln 1=n$.

D. Strong-coupling equations near FM-QCP

We now investigate the effect on superconductivity. The self-consistent 'strong-coupling' equations for the 4 4 matrix Matsubara Green functions G and self-energies are

$$G_{nk} = T \sum_n \int_p \left[V_{m,n}^c G_{k,p}^c + V_{m,n}^s G_{k,p}^s \right] \quad (13)$$

$$G_{nk} = (i^n 1 - k^2 - n^2)^{-1} \quad (14)$$

where \int_n and \int_p are suitable generalizations of Pauli matrices.²⁵ These equations take into account both the scattering and pairing effects of the phonon-mediated interaction V^c and the spin-uctuation-mediated-interaction V^s (although they neglect vertex corrections). The self-energy equation is represented diagrammatically in Fig. 2. For isotropic superconductivity with interactions in charge and spin channels the strong-coupling equations reduce to the following frequency-

dependent, momentum-independent form :

$$\bar{G}_m = \bar{G}_m^0 + T \sum_n V_{m-n}^+ G_n \quad (15)$$

$$e_m = T \sum_n V_{m-n} F_n \quad (16)$$

$$G_n = \frac{\bar{G}_n}{\bar{G}_n^2 + e_n^2} \quad (17)$$

$$F_n = \frac{e_n}{\bar{G}_n^2 + e_n^2} \quad (18)$$

where $V_n = V_n^c - V_n^s$, and G_n, F_n, \bar{G}_n, e_n are the momentum-integrated ordinary and anomalous Green functions and selfenergies.

E. Abrikosov-Gor'kov equations near FM-QCP

In the vicinity of the QPT, where β is small, V_n^s is dominated by the divergence at small β_n . Now, V_n^s is sampled at discrete bosonic Matsubara frequencies $\beta_n = 2\pi T(n+1/2)$. If the first nonzero Matsubara frequency, $\beta_1 = 2\pi T$, is much larger than the frequency cutoff β_D , we can discard all nonzero Matsubara frequencies. This corresponds to replacing the dynamic interaction V_n^s by a static one, $V_n^s \rightarrow V_0^s$. The spin fluctuations are now characterized by a single number, V_0^s . From Eqs. (11) and (12),

$$V_0^s = J \frac{0}{k_F} \frac{0}{k_F} \quad (2D \text{ model}); \quad (19)$$

$$V_0^s = \frac{J}{2} \frac{0}{k_F} \ln \frac{2k_F}{\beta_D} \quad (3D \text{ model}); \quad (20)$$

Let us also replace the dynamic, phonon-mediated interaction by a BCS-type interaction ($V_n^c = V^{BCS}$), with a frequency cutoff β_D of the order of the Debye frequency. Then Eqs. (15) and (16) simplify to

$$\bar{G}_n = \bar{G}_n^0 + T V_0^s G_n \quad (21)$$

$$e_n = T \sum_m V^{BCS} F_m - T V_0^s F_n \quad (22)$$

Compare these with the case of static charge and spin disorder²⁶, that is, magnetic impurities in a superconductor. That system can be described by the BCS model with additional random delta-correlated potentials $U^c(x)$ and $U^s(x)$ in the charge and spin channels, whose variances are W^c and W^s in the sense that $\langle U^c(x) U^c(x') \rangle = W^c \delta(x-x')$ and $\langle U^s(x) U^s(x') \rangle = W^s \delta(x-x')$:

$$S^{AG}[\bar{G}; U^c; U^s] = T \sum_n \sum_k (i\bar{G}_n^0 - k)_{nk} \bar{G}_n^0 + \frac{1}{2} V^{BCS} \sum_x \sum_x U^c(x) \sum_x U^s(x) S_{xi} \quad (23)$$

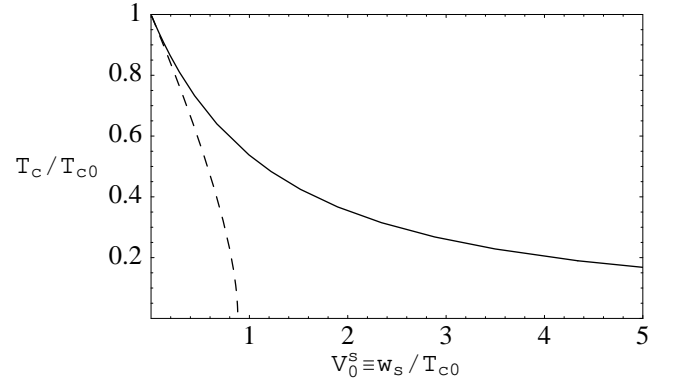


FIG. 3: Suppression of T_c by static magnetic disorder of strength w^s (dashed line) and by quasi-static spin fluctuations of strength V_0^s (solid line).

Let $w^{c/s} = 2\pi W^{c/s} = 1/c_{FS}$, where c_{FS} are the ordinary and spin- $\uparrow\downarrow$ scattering times, and β_D is the density of states at the Fermi energy. Define $w^s = w^c - w^s$. One then obtains the Abrikosov-Gor'kov equations

$$\bar{G}_n = \bar{G}_n^0 + \frac{w^+}{2} G_n \quad (24)$$

$$e_n = T \sum_m V^{BCS} F_m + \frac{w}{2} F_n \quad (25)$$

Comparing Eqs. (21) and (22) with (24) and (25) shows that the quasi-static spin-spin interaction V^s can effectively be replaced by static spin disorder whose strength $w^s = T V_0^s$ is temperature-dependent. The factor of T arises from the Matsubara frequency sum in the Eliashberg equations, and is necessary on dimensional grounds.

From Abrikosov-Gor'kov theory it is known that $T_c = T_{c0}$ depends only on w^s according to the following implicit equation²⁶:

$$\ln \frac{T_c}{T_{c0}} = \frac{1}{2} \left(\frac{1}{2} + \frac{w^s}{2 T_c} \right) \quad (26)$$

where T_{c0} is the critical temperature of the clean superconductor, and $\gamma(z)$ is the digamma function. In this scenario, T_c falls to zero when $w^s = \frac{-\gamma(0)}{2} = \frac{1}{2e} T_{c0}$ (Fig. 3, dashed line). A finite concentration of magnetic impurities is sufficient to destroy superconductivity. However, the extra factor of T in the spin-fluctuation scenario indicates that at lower temperatures there are fewer excitations and the depairing effect is less pronounced. Substituting in Eq. (26), we find

$$\ln \frac{T_c}{T_{c0}} = \frac{1}{2} \left(\frac{1}{2} + \frac{V_0^s}{2} \right) \quad (27)$$

This is an explicit equation for T_c which is even simpler than the AG result (Fig. 3, solid line)! The limiting form is

are

$$\frac{T_c}{T_{c0}} = 1 - \frac{V_0^s}{4} \quad \text{for } V_0^s \ll 0; \quad (28)$$

$$\frac{T_c}{T_{c0}} = \frac{1}{2e V_0^s} \quad \text{for } V_0^s \ll 1; \quad (29)$$

Superconductivity is only destroyed when the strength of the spin fluctuations becomes infinite. Inserting Eq. (19) or (20) into (29) gives

$$\frac{T_c}{T_{c0}} = \frac{1}{2e} \frac{1}{J} \frac{k_F}{0} \quad (2D); \quad (30)$$

$$\frac{T_c}{T_{c0}} = \frac{2}{2e} \frac{1}{J} \frac{k_F}{0} \ln \frac{2k_F}{0} \quad (3D); \quad (31)$$

In the immediate vicinity of the QCP, the bare inverse correlation length ξ_0 is a constant of the order of k_F , whereas the true inverse correlation length goes to zero according to some power law, $\xi \propto |J - J_c|^\nu$, as J approaches J_c . In Eqs. (30) and (31), the dimensionless quantities J and k_F/ξ_0 are constants of order unity, whereas the ratio ξ_0/ξ (which is the square root of the Stoner enhancement factor) becomes infinite. Hence, $T_c(J) \propto \frac{1}{\ln |J - J_c|}$ in 3D, and $J \propto |J - J_c|$ in 2D. Note that the fluctuations are more severe in 2D than in 3D, and T_c is more strongly suppressed. The quantum critical exponent affects the form of the 2D result but only the prefactor of the 3D result.

It is likely that $(J - J_c)$ is proportional to $(p - p_c)$, where p is an experimental control parameter such as pressure. Substituting p for J , we obtain predictions that can be compared with experiment.

In the limit $\xi_0 \rightarrow 0$, $1/\xi_0 \rightarrow \infty$ and ξ_0/ξ are always larger than ξ_0/ξ . Hence our initial assumption $2T_c \ll \xi_0/\xi$ is valid in the vicinity of the superconducting transition line. This justifies the working above a posteriori.

Farther away from the QCP, the other factors in Eqs. (30) and (31) may come into play. It is likely that changing the experimental parameter p has a significant effect not only on J , but also on the degree of nesting of the Fermi surface, and hence on ξ_0 . Then T_c will deviate from a pure logarithm or power law.

F. Phase diagram

In the presence of an externally applied exchange field, such as would arise from artificially polarized impurity spins, it is possible for superconducting order to exist. In fact, Larkin and Ovchinnikov¹¹ show that the exchange splitting h has no effect on T_c until it reaches about ≈ 2 . (The case of an externally applied magnetic field is more complicated due to orbital effects.)

The case for coexistence of superconductivity and spontaneous magnetization is a more difficult one. In a fully self-consistent mean-field theory, the superconducting order parameter and the magnetic order parameter

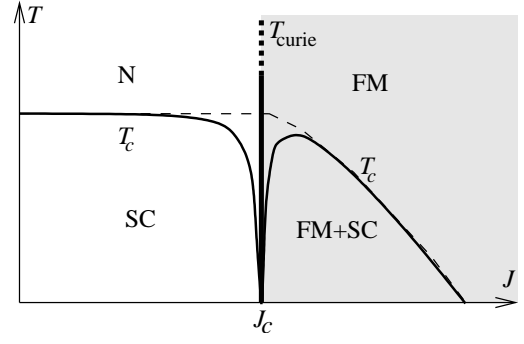


FIG. 4: Corrections to mean-field phase diagram due to fluctuations, assuming vertical FM phase boundary. N' represents the normal, non-magnetic metallic phase.

either M attempt to suppress each other. For a single-band model in which the same electrons take part in Cooper pairing and in Stoner itinerant ferromagnetism, the competition is so intense that the coexistence region in Fig. 4 is eliminated, leaving a first-order FM/SC phase boundary, terminating in a first-order QCP, and the analysis in this paper is not relevant. It may be possible, however, for FM and SC to coexist in multiband systems. In the following discussion, we presuppose coexistence of FM and SC at the mean-field level.

First let us assume that the magnetic phase boundary is vertical. On the left of this boundary, $M = 0$, so T_c should be constant (dashed line in Fig. 4). The magnetic fluctuations should suppress T_c to zero as described above (solid curve). On the right of the magnetic phase boundary, magnetic order is present, and T_c should be suppressed at the mean-field level. Suppose that the mean-field values of T_c are given by the dashed curve in Fig. 4. Now, since the equation for T_c is linear, the pair-breaking effect of FM order and FM fluctuations combine additively in the argument of the digamma function. Since the fluctuations are present on both sides of the transition, we expect that $T_c(J)$ is suppressed to zero as $J \rightarrow J_c$ from either direction (solid curve):

IV. EFFECT OF SDW FLUCTUATIONS ON T_c

A. q near an SDW-QCP

In order to treat a system close to a SDW instability, we must abandon the assumption of a spherical Fermi surface. A SDW system typically has a Fermi surface which is almost nested, meaning that there are portions of the Fermi surface which almost overlap when shifted relative to each other by a nesting vector Q . The spin fluctuations with wavevectors close to Q are the low-energy quantum critical fluctuations, and it is they that play an important role in suppressing superconductivity.

In order to proceed we need to choose a definite model for the Fermi surface. Let us begin with a 2D model.

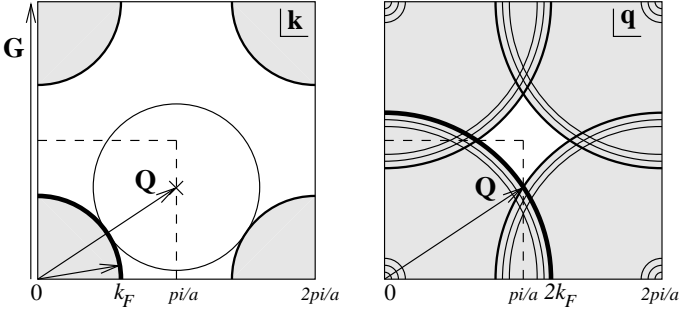


FIG. 5: (Left) Circular Fermi surface for $0 < k_x, k_y < \frac{2}{a}$. Solid gridlines indicate k -space unit cell boundaries; dashed lines indicate boundary of 1st Brillouin zone. Empty circle is image of Fermi surface under translation by Q . (Right) Contours of χ_q (schematic).

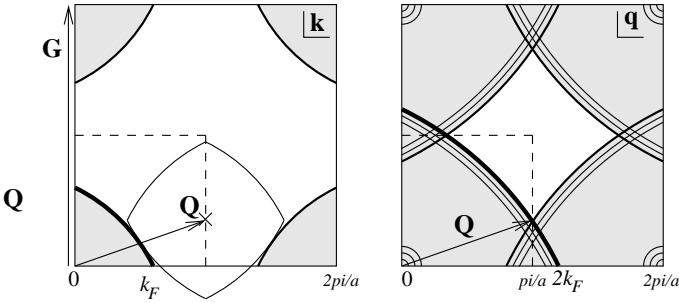


FIG. 6: Flattened Fermi surface. The line singularities in χ_q have a larger magnitude than before. The singularity at $q = 0$ also changes shape, but this is not shown, and is not relevant to the discussion.

Suppose the Fermi surface is a circle of radius k_F . Shifting this by $2k_F$ in any direction gives a circle tangent to the original circle, suggesting in perfect nesting. Now the anisotropy of the crystal comes into play. Since the Fermi surface typically occupies a sizeable fraction of the Brillouin zone, we must consider nesting between periodic images. In k -space, shifting the Fermi surface by Q makes it tangent to the original Fermi surface at two points rather than one.

It is useful to perform the analysis in q -space. The $1/q$ singularity in χ_q is still present, but there is a more relevant $1 = \frac{2k_F}{q}$ singularity on a circle of radius $2k_F$. This circle and its periodic images intersect at the point Q (and three other points related to Q by symmetry), and there χ_q is enhanced by a factor of 2. This construction, illustrated in Fig. 5, determines the optimal nesting vector²⁷. In summary, the radius of the Fermi surface determines the magnitude(s) of the nesting vectors, and the lattice anisotropy determines their direction(s).

Now suppose the Fermi surface undergoes ‘pincushion’ distortion, such that the circular arcs that make up the Fermi surface become flatter (Fig. 6). The optimal vector Q may change; more importantly, the ‘nesting’ singularities in χ_q become larger. Assuming that the Fermi velocity v_F and the density of states are not significantly

altered during the distortion,

$$\chi_q = \frac{m}{2k_F^2} \frac{1 - \frac{q}{2k_c}}{1 - \frac{q}{2k_c}} = \frac{m}{2k_F^2} \frac{q}{q} \frac{k_c}{q} \quad (32)$$

where q_\perp is the perpendicular distance from q to the Fermi surface in q -space (towards the center of the arc). The magnitude of the singularity increases with the square root of the radius of the curvature. Remember that this is enhanced by a factor of 2 where the singularities intersect. When $k_c = 1$ the Fermi surface becomes a square and $q_\perp = (q)$.

In the 3D analogue of this model, the Fermi surface consists of eight, approximately triangular, portions of spherical surfaces. As the radius of curvature of each portion is increased towards infinity, the Fermi surface morphs from a sphere to an octahedron:

$$\chi_q = \frac{m}{4k_F^3} \frac{2k_c^2 (1 - \frac{q}{2k_c})}{q} = \frac{m}{4k_F^3} \frac{(q)}{q} k_c \quad (33)$$

The discontinuity in χ_q is proportional to the radius of curvature.

B. Spin-spin interaction V_{nq}^s near an SDW $-QCP$

We also need an approximation for the spin-spin interaction V_{nq}^s . First consider the bare Green function G_{nq}^0 , given by

$$G_{nq}^0 = \frac{1}{i!} \frac{f(k)}{k} \frac{f(k+q)}{k+q+k} \quad (34)$$

This integral is somewhat similar to the expression for χ_q , Eq. (8). It is large when q is close to a nesting vector of the Fermi surface. In this case, the definition of ‘nesting’ is more stringent: portions of the Fermi surface overlap when shifted by the nesting vector Q , and the ‘empty’ side of one portion matches up with the ‘filled’ side of the other. Because of this, G_{nq}^0 does not have a peak near $q = 0$, unlike χ_q . We shall assume that both G_{nq}^0 and χ_q are peaked at the same wavevector Q . This is a reasonable assumption if the SDW and SC are caused by nesting of the same Fermi surface.

For small w and for q close to Q , G_{nq}^0 can be approximated by a Hertzian of width w . In this model, it is expected that G_{0q}^0 and G_{0Q}^0 will both depend upon the curvature parameter k_c . In particular, when k_c is large, the system is well nested, and G_{0Q}^0 is expected to be small.

$$G_{nq}^0 = \frac{G_{0Q}^0}{w^2 + \frac{1}{2} (Q - Q)^2 + \frac{1}{2} (n - n)^2} \quad (35)$$

Then, in V_{nq}^s , G_{0Q}^0 is replaced by the ‘renormalized’ inverse spin-fluctuation correlation length λ , which is smaller due to Stoner enhancement:

$$V_{nq}^s = \frac{J_0^2}{w^2 + \frac{1}{2} (Q - Q)^2 + \frac{1}{2} (n - n)^2} \quad (36)$$

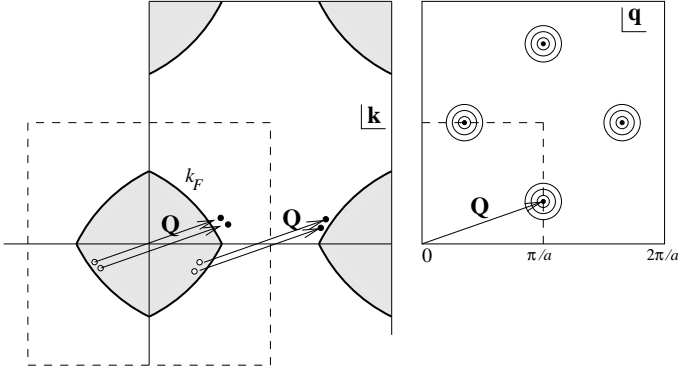


FIG. 7: (Left) Electron-hole excitations near the nesting vector which give the main contribution to V_0^s . (Right) Schematic contour plot of V_0^s (or V_0^s).

where $V_0^s = \frac{J_0^2}{2 + \frac{J_0^2}{J_c^2}} \frac{1}{Q^2}$. Ultimately, the FLEX calculation requires only the $n = 0$ component, which is a Lorentzian in q -space peaked at $q = Q$:

$$V_{0q}^s = \frac{J_0^2}{2 + \frac{J_0^2}{J_c^2}} \frac{1}{Q^2} \quad (37)$$

C. Effective interaction V_n^s near SDW-QCP; suppression of T_c

The momentum-averaged interaction is given, as before, by Eq. (7). Since V_q has a weaker divergence for the SDW case than for the FM case, V_0^s also has a weaker divergence, as we shall see below. First consider the 2D model. To do the integral over q , we use coordinates q_k and q_\perp oriented tangentially and perpendicularly to the Fermi surface. There is a factor of 2 arising from the overlap of two singularities.

$$\begin{aligned} V_n^s &= \frac{1}{(2\pi)^2} \int_{k_F}^Z d^2q V_{nq}^s \\ &= \frac{1}{(2\pi)^2} \int_{k_F}^Z dq_\perp \int_{k_F}^Z dq_k \frac{m}{2k_F^2} \frac{1}{(q_\perp^2 + k_C^2)^2} \\ &= \frac{1}{(2\pi)^2} \int_{k_F}^Z dq_\perp \int_{k_F}^Z dq_k \frac{m}{2k_F^2} \frac{1}{(q_\perp^2 + k_C^2)^2} \\ &= \frac{1}{(2\pi)^2} \int_{k_F}^Z dq_\perp \int_{k_F}^Z dq_k \frac{m}{2k_F^2} \frac{1}{(q_\perp^2 + k_C^2)^2} \\ &= \frac{1}{(2\pi)^2} \int_{k_F}^Z dq_\perp \int_{k_F}^Z dq_k \frac{m}{2k_F^2} \frac{1}{(q_\perp^2 + k_C^2)^2} \\ &= \frac{1}{(2\pi)^2} \int_{k_F}^Z dq_\perp \int_{k_F}^Z dq_k \frac{m}{2k_F^2} \frac{1}{(q_\perp^2 + k_C^2)^2} \\ &= \frac{1}{(2\pi)^2} \int_{k_F}^Z dq_\perp \int_{k_F}^Z dq_k \frac{m}{2k_F^2} \frac{1}{(q_\perp^2 + k_C^2)^2} \\ &= \frac{1}{(2\pi)^2} \int_{k_F}^Z dq_\perp \int_{k_F}^Z dq_k \frac{m}{2k_F^2} \frac{1}{(q_\perp^2 + k_C^2)^2} \end{aligned} \quad (38)$$

At zero frequency,

$$V_0^s = \frac{J_0^2}{k_F^2} \frac{1}{k_C^2} \quad (39)$$

The strength of the effective interaction increases when the Fermi surface becomes flatter or when the coupling J is tuned towards J_c . In general, V_0^s goes to zero at the QCP whereas k_C is large but finite. Therefore, near the QCP, $V_0^s \propto 1/k_C^2$, and by the arguments of the previous sections, the superconducting T_c is suppressed as

$$T_c \propto \frac{1}{(J - J_c)^2} \quad (40)$$

The quantity $J - J_c$ is of order unity, but V_0^s is likely to be small, as explained earlier. Hence the suppression of T_c is much weaker for the SDW case than for the FM case.

For the 3D model, an estimate gives

$$\begin{aligned} V_n^s &= \frac{1}{(2\pi)^3} \int_{k_F}^Z d^3q V_{nq}^s \\ &= \frac{1}{(2\pi)^3} \int_{k_F}^Z dq_\perp \int_{k_F}^Z dq_k \frac{m}{4k_F^3} \frac{1}{(q_\perp^2 + k_C^2)^2} \\ &= \frac{1}{(2\pi)^3} \int_{k_F}^Z dq_\perp \int_{k_F}^Z dq_k \frac{m}{4k_F^3} \frac{1}{(q_\perp^2 + k_C^2)^2} \\ &= \frac{1}{(2\pi)^3} \int_{k_F}^Z dq_\perp \int_{k_F}^Z dq_k \frac{m}{4k_F^3} \frac{1}{(q_\perp^2 + k_C^2)^2} \\ &= \frac{1}{(2\pi)^3} \int_{k_F}^Z dq_\perp \int_{k_F}^Z dq_k \frac{m}{4k_F^3} \frac{1}{(q_\perp^2 + k_C^2)^2} \\ &= \frac{1}{(2\pi)^3} \int_{k_F}^Z dq_\perp \int_{k_F}^Z dq_k \frac{m}{4k_F^3} \frac{1}{(q_\perp^2 + k_C^2)^2} \\ &= \frac{1}{(2\pi)^3} \int_{k_F}^Z dq_\perp \int_{k_F}^Z dq_k \frac{m}{4k_F^3} \frac{1}{(q_\perp^2 + k_C^2)^2} \end{aligned} \quad (41)$$

The integral is not divergent at small q_\perp , so V_0^s remains finite, and T_c is not suppressed to zero. In fact, since $\frac{1}{k_F^2}$ is small, the suppression should be a small effect. Taking into account the terms of order J_c^2 , we see that $V_0^s \propto \text{const} - \frac{J_c^2}{J^2}$, so $T_c \propto \text{const} - \frac{J_c^2}{J^2}$: the critical temperature has a cusp near the QCP.

The above arguments apply close to the QCP. Farther away from the QCP, the variation of V_0^s may be significant. In fact, it is likely that the quantum phase transition is caused by an increase in nesting, so V_0^s decreases as the QCP is approached from far. Then the argument implies that T_c should increase at first as the QCP is approached. This can be justified as follows: although Fermi-surface nesting causes an enhancement of V_0^s and J , and indirectly enhances the V^s , it also narrows the peak in the interaction in q -space so that the magnetism competes less effectively for the Fermi surface. Of course, this result is model-dependent.

V. NUMERICAL RESULTS

Figure 8 shows numerical results obtained by self-consistent solution of Eqs. (15)–(18), using an Einstein

phonon model for V_n^c and the various approximations derived above for V_n^s . From the log-log plot (Fig. 8(b)) it is clear that T_c obeys the expected power laws ($\propto p^{-1}$ and p^{-2}) near a 2D FM or AF transition respectively, and that in 3D the suppression of T_c is very weak.

V I. D I S C U S S I O N

We have made predictions about the analytic behavior of the T_c of an isotropic superconductor near ferromagnetic or spin-density-wave QCPs:

2D FM	T_c	$p - \sqrt{J} \sqrt{J}$
2D SDW	T_c	$\sqrt{J} \sqrt{J}^2$
3D FM	T_c	$1 = \ln(1 -) \quad 1 = \ln(1 - \sqrt{J} \sqrt{J})$
3D SDW	T_c	$\text{const} + \sqrt{J} \sqrt{J}$

T_c is suppressed all the way to zero by ferromagnetic quantum critical fluctuations in 2D and 3D, even before magnetic order sets in. Spin-density-wave fluctuations have a weaker effect; in 2D they can suppress T_c to zero, but in 3D they merely produce a cusp. These predictions rely on the assumption of coexistence of magnetism and homogeneous, isotropic superconductivity at the mean-field level. The results for the 3D FM should be contrasted with the prediction in the p-wave case of a finite T_c at the QCP.¹⁷

These results are based on the theory of Abrikosov and Gor'kov, which has undergone several refinements since its publication in 1961. Calculations including higher-order scatterings from a classical spin^{28,29,30} and non-perturbative studies³¹ suggest that magnetic impurities lead to states within the superconducting gap; however, the predicted T_c (which is all that matters to our conclusions) is not qualitatively different from that of Abrikosov and Gor'kov. Taking the quantum nature of the spins into account³² suggests that the spins are quenched by the Kondo effect at low temperatures (in the case of antiferromagnetic exchange $J > 0$), and thus cease to cause pair-breaking, so that superconductivity is destroyed only at an infinite concentration of magnetic impurities. However, the present paper deals not with impurity spins but with quantum critical spin fluctuations: in a nearly magnetic metal these are not destroyed at low temperatures by any Kondo effect, so there is no reason to expect such a phenomenon in a nearly magnetic superconductor.

We are not aware of any experimental systems where a FM QCP has been seen in a phonon-mediated superconductor. But, as Saxena et al remark in Ref.⁵, very few itinerant-electron ferromagnets studied to date have

been prepared in a sufficiently pure state, or have been 'tuned', to be sufficiently close to the border of ferromagnetism, or cooled to sufficiently low temperatures, to provide a definitive check of the predictions of theory.

In Fe³³, signs of superconductivity have been observed on the high-pressure side of a first-order structural phase transition, but it is unclear if this is (i) conventional phonon-mediated superconductivity which is suppressed by ferromagnetism in the bcc phase and revealed in the hcp phase, (ii) unconventional superconductivity mediated by ferromagnetic spin fluctuations, or (iii) by some other type of spin fluctuation present in the hcp phase. As the transition is first-order, the analysis in this paper is not applicable.

The compound MgCNi₃ is a superconductor below 8K³⁴, with a BCS-like (s-wave-like) specific heat, and there has been a theoretical prediction that it is unstable to ferromagnetism upon doping with 12% Na or Li. Such a ferromagnetic quantum critical point may be a testing ground for this theory.

In ErRh₄B₄⁷ and HoMo₆S₈^{8,9} the FM state destroys superconductivity at sufficiently low temperatures, whereas at intermediate temperatures the coexistence gives rise to a compromise oscillatory behavior. The physics here is dominated by orbital diamagnetism, rather than by paramagnetic spin fluctuations.

The rare-earth nickel borocarbides³⁵ show coexisting SDW and superconductivity, as well as corresponding nesting features in the Fermi surface.³⁶ Suppression of T_c using hydrostatic and chemical pressure to manipulate the exchange interaction has been reported³⁷ but the AFM QCP has not been explored.

In the Bechgaard salt (TM TSF)₂PF₆, pressure has been used to tune the SDW state through a QCP at 6.4 kbar where a superconducting state is found. The quasi-2D BEDT-TTF salts have a high superconducting temperature and are near the boundary of an AF insulating phase.³⁸ However, the character and mechanism of superconductivity in these organic materials is still debated, and thus the applicability of our model is in doubt.

To conclude, while there are several candidate model systems with which to test these predictions, up to now no sufficiently detailed studies have been performed.

A c k n o w l e d g m e n t s

It is a pleasure to thank A. Nevidomskyy for helpful discussions. Y. L. L. thanks Trinity College, Cambridge for financial support.

¹ K. Miyake, S. Schmitt-Rink, and C. M. Varma, Phys. Rev. B (Rapid Communication) 34, 6554 (1986).

² P. W. Anderson and P. Morel, Phys. Rev. 123, 1911

(1961).

³ R. Balian and N. R. Werthamer, Phys. Rev. 131, 1553 (1963).

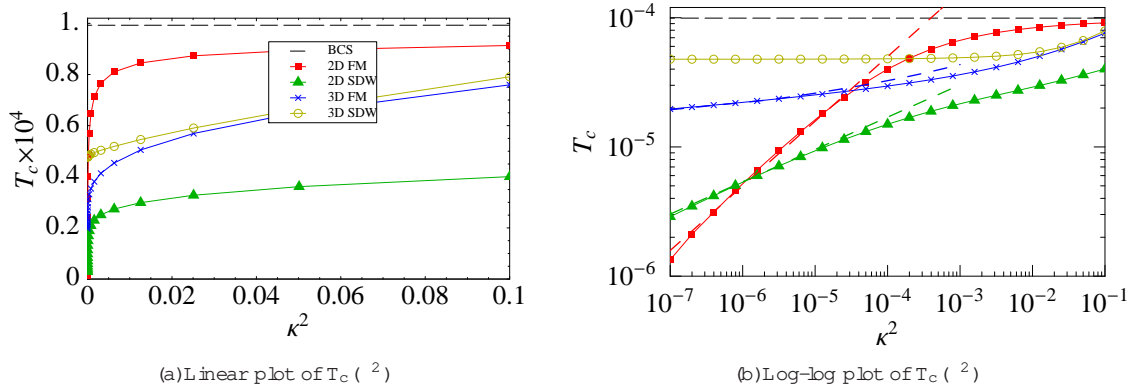


FIG. 8: Numerical results for superconducting T_c as a function of distance from quantum critical point κ^2 for suitable model parameters, obtained using an imaginary-time Eliashberg approach.

- ⁴ Y. Maeno, H. Hashimoto, K. Yoshida, S. Nishizaki, T. Fujita, J. G. Bednorz, and F. Lichtenberg, *Nature* 372, 532 (1994).
- ⁵ S. S. Saxena et al., *Nature* 406, 587 (2000).
- ⁶ S. S. Saxena and P. B. Littlewood, *Nature* 412, 290 (2001).
- ⁷ W. A. Fertig, D. C. Johnston, L. E. DeLong, R. W. McCallum, M. B. Maple, and B. T. Matthias, *Phys. Rev. Lett.* 38, 987 (1977).
- ⁸ J. W. Lynn, G. Shirane, W. Thomson, and R. N. Shelton, *Phys. Rev. Lett.* 46, 368 (1981).
- ⁹ J. W. Lynn, G. Shirane, W. Thomson, and R. N. Shelton, *Solid State Commun.* 23, 37 (1977).
- ¹⁰ L. P. Gor'kov and A. I. Rusinov, *Sov. Phys. JETP* 19, 922 (1964).
- ¹¹ A. I. Larkin and Y. N. Ovchinnikov, *Sov. Phys. JETP* 20, 762 (1965).
- ¹² P. Fulde and R. A. Ferrell, *Phys. Rev.* 135, A550 (1964).
- ¹³ G. B. Il'bro and W. L. McMillan, *Phys. Rev. B* 14, 1887 (1976).
- ¹⁴ N. S. Saravananuttu (2003), private communication.
- ¹⁵ N. F. Berk and J. R. Schrieffer, *Phys. Rev. Lett.* 17, 433 (1966).
- ¹⁶ P. Monthoux and D. Pines, *Phys. Rev. Lett.* 69, 961 (1992).
- ¹⁷ Z. Wang, W. Mao, and K. Bedell, *Phys. Rev. Lett.* 87, 257001 (2001).
- ¹⁸ R. Roussev and A. J. Millis, *Phys. Rev. B* 63, 140504(R) (2001).
- ¹⁹ Q. Li, D. Belitz, and T. R. Kirkpatrick, *Phys. Rev. B* 74, 134505 (2006).
- ²⁰ W. L. McMillan and J. M. Rowell, *Phys. Rev. Lett.* 14, 108 (1964).
- ²¹ J. A. Hertz, *Phys. Rev. B* 14, 1165 (1976).
- ²² D. Belitz, T. R. Kirkpatrick, and T. Vojta, *Phys. Rev. Lett.* 82, 4707 (1999).
- ²³ D. Belitz, T. R. Kirkpatrick, and T. Vojta, *Rev. Mod. Phys.* 77, 579 (2005).
- ²⁴ J. Rech, C. Pepin, and A. V. Chubukov, Quantum critical behavior in itinerant electron systems { Eliashberg theory and instability of a ferromagnetic quantum-critical point.
- ²⁵ K. Maki, in *Superconductivity*, edited by R. D. Parks (Marcel Dekker, Inc., NY, 1969), vol. 2, chap. 18.
- ²⁶ A. A. Abrikosov and L. P. Gor'kov, *Sov. Phys. JETP* 12 (1961).
- ²⁷ P. B. Littlewood, J. Zaanen, G. Aeppli, and H. Monien, *Phys. Rev. B* 48, 487 (1993).
- ²⁸ L. Yu, *Acta Phys. Sinica* 21, 75 (1965).
- ²⁹ H. Shiba, *Prog. Theor. Phys.* 40, 435 (1968).
- ³⁰ A. I. Rusinov, *JETP Lett.* 9, 85 (1969).
- ³¹ A. Lamacraft and B. D. Simons, *Phys. Rev. B* 64, 014514 (2001).
- ³² E. Muller-Hartmann and J. Zittartz, *Phys. Rev. Lett.* 26, 428 (1971).
- ³³ K. Shimizu et al., *Nature* 412, 316 (2001).
- ³⁴ J.-Y. Lin et al., *Phys. Rev. B* 67, 052501 (2003).
- ³⁵ R. J. Cava et al., *Nature* 367, 252 (1994).
- ³⁶ S. B. Dugdale, M. A. Alam, I. Wilkinson, R. J. Hughes, I. R. Fisher, P. C. Canfield, T. Jarlborg, and G. Santi, *Phys. Rev. Lett.* 83, 4824 (1999).
- ³⁷ H. Michor, M. ElHagary, L. Naber, E. Bauer, and G. Hilscher, *Phys. Rev. B* 61, R6487 (2000).
- ³⁸ H. A. Kutsu, K. Saito, and M. Sorai, *Phys. Rev. B* 61, 4346 (2000).
- ³⁹ Strictly speaking, the angular momentum classifications s, p, d should be replaced by the appropriate representations of the symmetry group of the crystal.
- ⁴⁰ The Stoner model described above exhibits a quantum critical point and a vertical FM phase boundary. The standard Heisenberg model, however, gives a finite-temperature phase transition whose Curie temperature is proportional to J .
- ⁴¹ Eq. (11) is not a truncated series expansion but rather an approximate form with the correct limiting behavior at small n and large n .